



## SYNTHESIS OF Mg-DOPED n(ZnO) THIN FILMS USING SOL-GEL & DIP-COATING METHOD AND CHARACTERIZATION OF ITS STRUCTURAL AND OPTICAL PROPERTIES

Archana Kumari Singh, Satya Pal Singh\*, Aman Alexander

Condensed Matter Physics & Nanoscience Laboratory, Department of Physics and Material Science of Madan Mohan Malaviya University of Technology, Gorakhpur, Uttar Pradesh, India

\*Corresponding author: [singh.satyapal@hotmail.com](mailto:singh.satyapal@hotmail.com)

Received: 06-02-2022; Revised & Accepted: 11-05-2022; Published: 31-05-2022

© Creative Commons Attribution-NonCommercial-NoDerivatives 4.0 International License <https://doi.org/10.55218/JASR.202213412>

### ABSTRACT

Mg-doped ZnO alloy thin films having hexagonal Wurtzite structures were prepared using the Sol-Gel method. The doping results into, increased surface roughness and reduced grain size. Photonic applications are made easier by altering the optical bandgap of ZnO nano-structured thin films doped with various components. Mg metal atom doped ZnO films are an excellent example for study. In this work, the thin film of Mg-doped ZnO is formed on glass substrate via dip coating method with varied concentration of dopant. Dip-coating method is one of the cheapest methods. SEM, Raman spectroscopy and UV-vis spectroscopy are used to characterize the thin films. The spectroscopic analysis revealed a more uniformed crystalline nano-structured surface with fewer structural defects. As the Mg atom concentration is increased, the results show a linear increment in the band gap of Mg-doped ZnO thin film in comparison to the pure ZnO nanostructured thin film, as well as there occurs an improvement in crystalline character. The reduction in intensity of visible radiation (enhancement in radiation in UV region) with increase in Mg concentration indicates for a decrease in intrinsic defects. The changing trends in optical and structural parameters as with increased Mg content reveal a non-linear and non-monotonic relations. The work provides insights to analyse the dependence of optical bandgap on crystal structure and defects.

**Keywords:** Thin-nano film, Mg-doped ZnO, Band gap, Sol-gel method, Dip coating method.

### 1. INTRODUCTION

Thin films of zinc oxide (ZnO) are used as transparent conducting films in variety of opto-electronic devices. Zinc Oxide (ZnO) is a II-VI compound and a n-type semiconductor having a large bandgap energy (3.37 eV at 300 K) and huge exciton binding energy (60 meV). Its hexagonal unit cell has lattice constants of  $a = b = 0.325$  nm and  $c = 0.521$  nm. Because of its wider bandgap, it is well suited for application as solar cell window layers, heat mirrors, liquid crystal displays and other photonic applications requiring a higher direct bandgap [1-8]. The higher bandgap is required for the short wavelength applications. However, the application of ZnO into integrated optical devices is limited due to their too narrow band gap [3, 7-9]. Doping Mg in ZnO produces a wider bandgap than ZnO, because of the reasons; it is widely used in ultraviolet optoelectronic devices [7].

Furthermore, adding ZnO to a chalcopyrite-based solar cell's window layer can increase the cell's overall efficiency by lowering absorption losses. It is been proven in the case for Mg-doped ZnO thin film. MgO has a NaCl-type cubic structure with a greater bandgap than ZnO, which has a wurtzite crystalline structure.

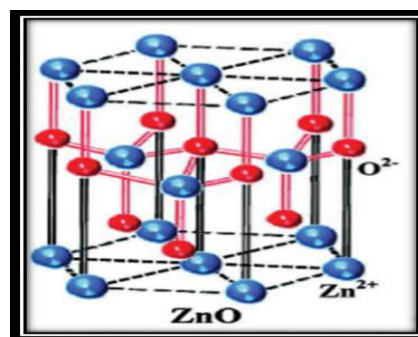


Fig. 1: Structure of ZnO

A feasible way to change the bandgap is to shift the Fermi-energy level by introducing impurity or doping atoms of a suitable element. Since dopant atoms of alike radius are recommended to produce such compounds with small lattice distortion,  $\text{Mg}^{2+}$  ions with radii 0.57 Å is found as one of the suitable elements for replacing  $\text{Zn}^{2+}$  ions with comparable radii of 0.60 Å. It makes Mg an acceptable dopant that can restore Zn atom in the lattice in ZnO with less lattice distortions. The elements of groups 2<sup>nd</sup> and 3<sup>rd</sup> have comparable radii to  $\text{Zn}^{2+}$  e. g.  $\text{Be}^{2+}$ ,  $\text{Mg}^{2+}$ ,  $\text{Ca}^{2+}$ , and  $\text{Cd}^{2+}$  [5-6, 10-13].

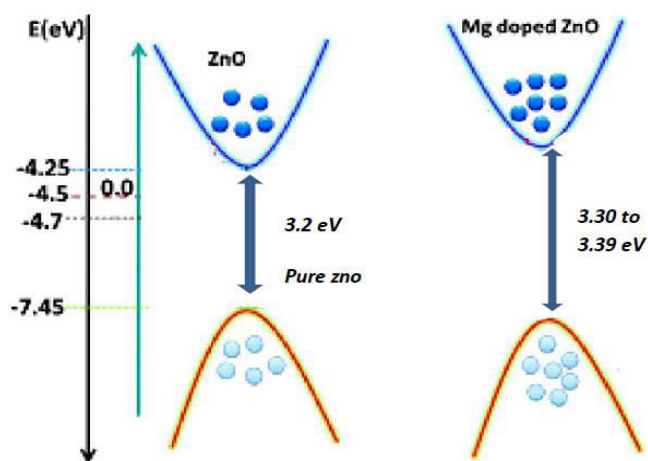


Fig. 2: Widening of bandgap by doping Mg content in pure ZnO

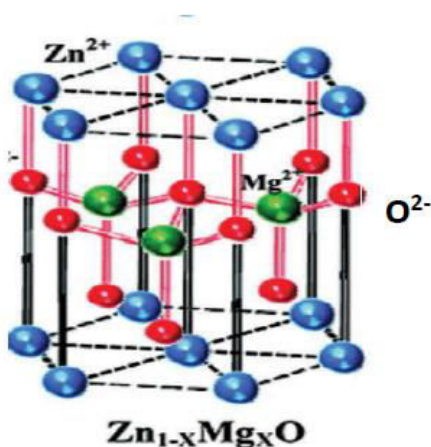


Fig. 3: Mg-doped ZnO Structure

Since structural parameters have a major impact on optical properties of materials, a thorough research on structural and optical parameters is required to get specific thin film properties that are desirable for photonic and optoelectronic applications. Furthermore, inclusion of Mg into ZnO has been shown to reduce

interstitial oxygen voids and electron density [14-16]. As a result, Mg doping has a significant impact on the optic properties of ZnO, and it also paves the way for tunable optical band-gaps. Mg-doped ZnO nano-structured thin films can be prepared in a variety of ways including Atomic Layer Deposition (ALD), Spray Pyrolysis, Plasma Enhanced Chemical Vapor Deposition (PECVD), Metal Organic Chemical Vapor Deposition (MOCVD), Molecular Beam Epitaxy (MBE), Electron Beam Evaporation, Pulsed Laser Deposition (PLD), Solgel Method etc.

Each of these techniques has different advantages. Among these techniques, sol-gel process allows a better control of the whole reactions during the synthesis of new material, and has other major advantages e. g. it is cheap and requires simple equipment. However, structural and optical properties of thin films are affected by growth process, precursors, temperature, dopant concentration, and so on. The properties also depend on the method of preparation of samples. In this work, we produce Mg-doped ZnO films with three different concentrations of Mg (0.95 wt%, 1.50 wt% and 2.12 wt% of Zn content) on the glass substrate by a combination of sol-gel and dip-coating method. We analyze its optical and structural properties using SEM, Raman Spectroscopy and UV-vis Spectroscopy, and correlate them.

## 2. EXPERIMENTAL

In this synthesis, zinc acetate dehydrate ( $\text{Zn}(\text{CH}_3\text{COO})_2 \cdot 2\text{H}_2\text{O}$ ), 2-methoxy ethanol ( $\text{C}_3\text{H}_8\text{O}_2$ ) and mono-ethanolamine ( $\text{C}_2\text{H}_7\text{NO}$ ) were taken as a solvent material, precursor, and solution stabilizer, respectively. Magnesium acetate-4-hydrate ( $(\text{CH}_3\text{COO})_2\text{Mg} \cdot 4\text{H}_2\text{O}$ ) was taken as a doping compound. First, a 0.5 M ZnO solution was prepared by rendering 5.49 gm of hydrated zinc acetate in 50 ml of 2-methoxy-ethanol using magnetic stirrer rigorously for 20 minutes at room temperature (300 K). Thereafter, different amount of doping compounds were added; here we doped magnesium with concentrations 0.95 wt% (0.17 gm), 1.50 wt% (0.27 gm) and 2.12 wt% (0.38gm) using magnesium acetate to the 0.5 M ZnO solutions. We placed the solution on magnetic stirrer at a constant speed of 800 RPM for 30 minutes at 75°C and thereafter mono ethanolamine was added dropwise maintaining the molar ratio 1:1 till the solution became clear. After getting a clear homogeneous solution, the mixture was stirred rigorously at constant speed for 2 hours. The solution was left in a closed beaker for 24 hours at room temperature [17-20]. Schematic representation of sol-gel

method adopted in this work is shown in Fig. 4. The glass slide was cleaned with acetone very well before going through the dip coating method (DCM). The glass slide was dip in the solution, and taken it vertically out, which drained the extra solution on the glass slide, and pre-heated the glass-slides at 100°C in hot air oven for 10 minutes as shown in Fig. 5. The same process of layering was repeated (coating) for 4 times [21-26]. At last, annealing was done in conventional muffle furnace at 500°C for 2 hours [18].

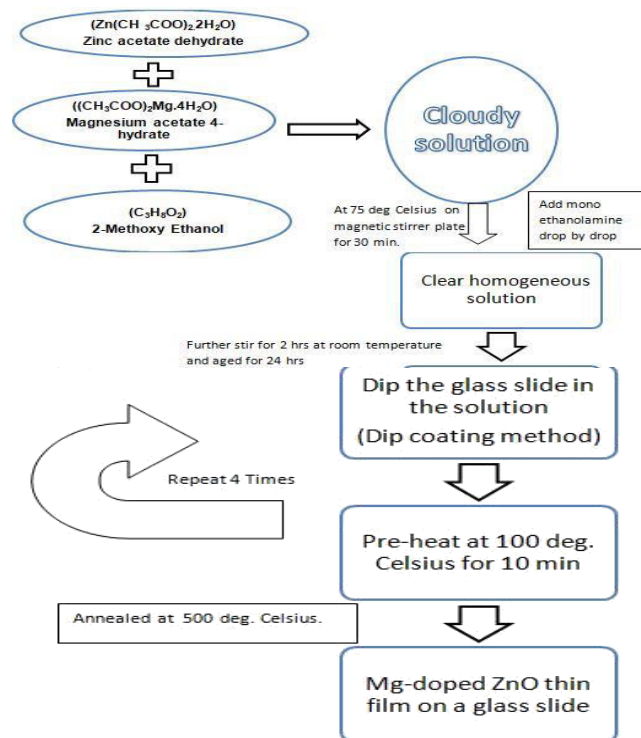


Fig. 4: Schematic Representation of Sol-Gel Method

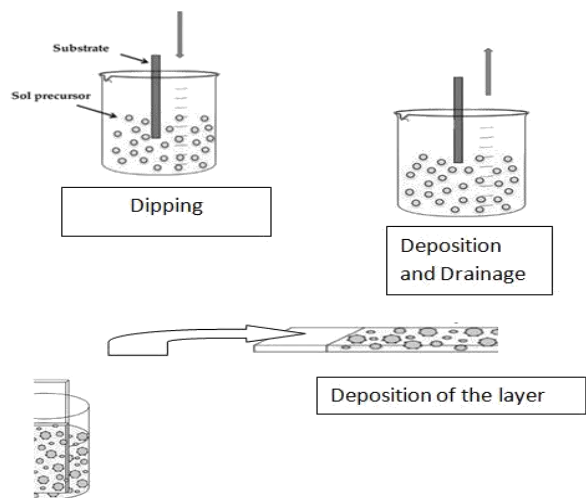


Fig. 5: Thin film coating process (Layering Process)

### 3. RESULTS AND DISCUSSION

#### 3.1. UV-Vis Spectroscopy

The study of absorption spectra in ultraviolet and nearby visible parts of the electromagnetic spectrum is known as UV-vis spectroscopy (sometimes also referred as UV/vis). This means that it uses visible and neighboring wavelength ranges of light. Electronic transitions occur in this region between different states of atoms and molecules. Fluorescence and absorption spectroscopy are complimentary to each other; fluorescence studies electron transitions from excited to ground state, whereas absorption studies transition from the ground to the excited state. Optical absorbance measurements of the samples were taken in the wavelength range of 210 nm to 390 nm. Because of the reasons, absorption coefficients depend on the properties of respective materials and the wavelength of light used. The absorption coefficient may be calculated using the following equation,  $\alpha = (2.303 A) / t$  where, A and t shows absorbance and film thickness, respectively.

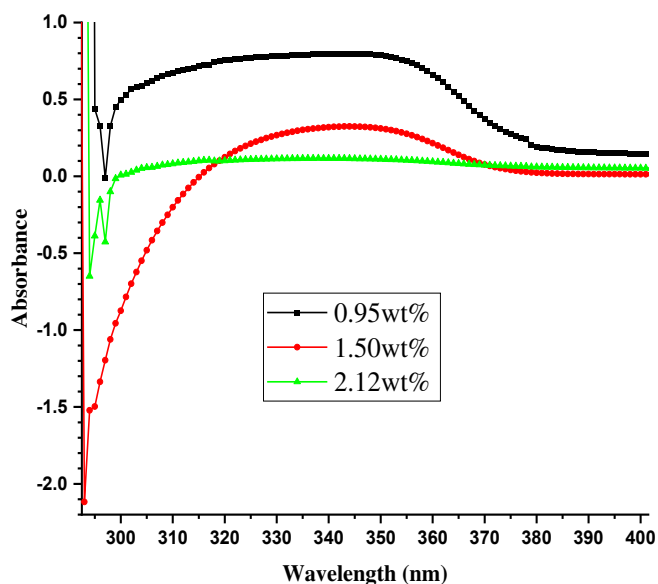


Fig. 6: Absorption spectra of Mg-doped ZnO

The UV-vis absorption spectra of Mg-doped ZnO nano-structured thin films on glass substrates are shown in Fig. (6). Each sample's absorption spectrum reveals good extent of absorption in the UV region at the edge of visible end. It shows nearly transparent behavior in the visible region [4]. Within the visible spectrum, all samples have a higher uniform transmittance level. Because of doping of Mg, the enhanced transmittance can be attributed to and the formation of a relatively smoother film. Furthermore, all of the samples, exhibit a

sharp cut-off at the ultraviolet (UV) region around 295 nm wavelength, indicating for high UV light absorption. The negative absorption coefficient can be accounted only on the basis of elastic scattering or because of partial contribution due to reflection of light from glass surface due to systematic errors associated with experiments. Though, latter one is ruled out, because the characterization was done by expert professionals at high-tech laboratory. There is a more feasible explanation for the negative absorption. The sample is first excited upon throwing light over it and emit light in presence of the surrounding environment. This could be because light excites samples from ground states to the lower excited states, whereas it comes back to ground states or the lower molecular orbitals from high energy molecular states, resulting into a positive emission rather than a net absorption yielding  $A < 0$ . The light source interacts with the samples, causing them to emit additional energy, resulting into emergent light greater than incident light. Because of their particular absorption properties as discussed earlier, Mg-doped-ZnO has gotten wider applications in detection of UV radiation.

### 3.2. Raman Spectroscopy

Raman spectroscopy is a noncorrosive technique that offers information about phase, chemical structure & polymorphicity, crystallinity and molecular interactions of the samples. It works on the principle of interaction of light with chemical bonds inside material as shown in Fig. (7). The scattered light retaining original wavelength does not give useful information and is known Rayleigh scattering. However, a very small fraction of incident

light (typically one out of  $10^9$ ) is scattered at distinct wavelengths (i. e. colors), which rely on the chemical structure of the analyte, this physical process is known as Raman Scattering. The results of our measurements are graphically represented as Raman spectra for different concentrations of magnesium doped in ZnO films. We plot frequency at X-axis, and the intensity of scattered light Y-axis. Frequency is measured in a unit known as the wavenumber  $\text{cm}^{-1}$ .

Typically, the peaks fall in the range of 500 to 2000  $\text{cm}^{-1}$ , and only appear if frequency associated with the vibrational modes match with the laser wavelength used. The non-resonant Raman spectra of the  $\text{Mg}_x\text{Zn}_{1-x}\text{O}$  nanoparticles for different doping concentrations of Mg i.e. 0.95 wt%, 1.50 wt%, and 2.12 wt% at room temperature and excited by 532 nm laser light, are shown in Fig. (8), Fig. (9) and Fig. (10), respectively.

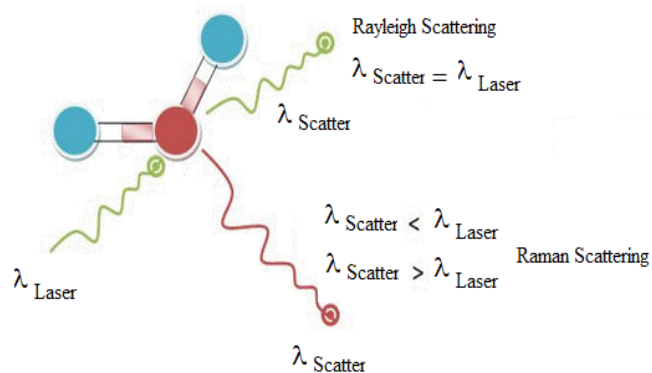


**Fig. 7: Schematic representation of basic principle of Raman scattering**

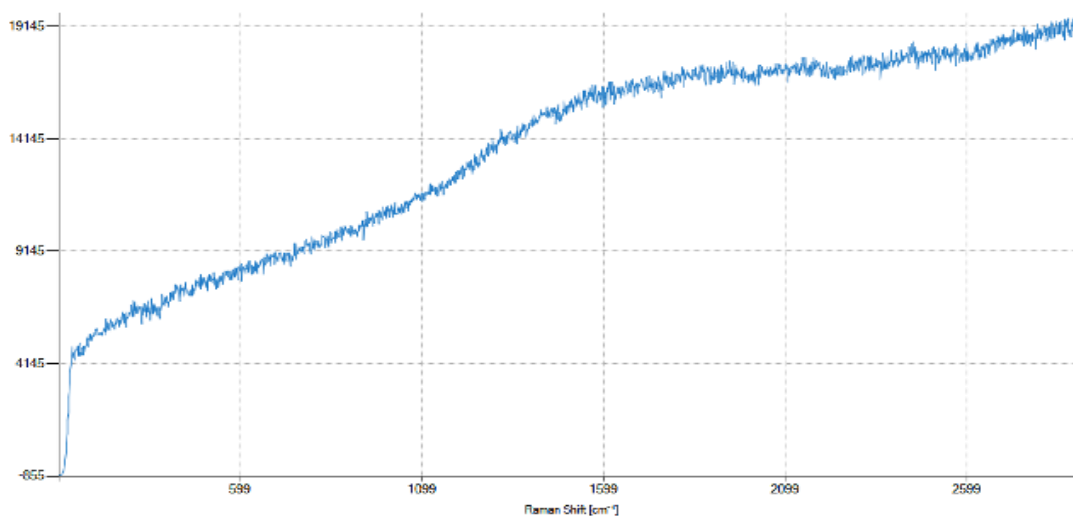


**Fig. 8: Raman spectroscopy of 0.95wt% Mg doped ZnO film**

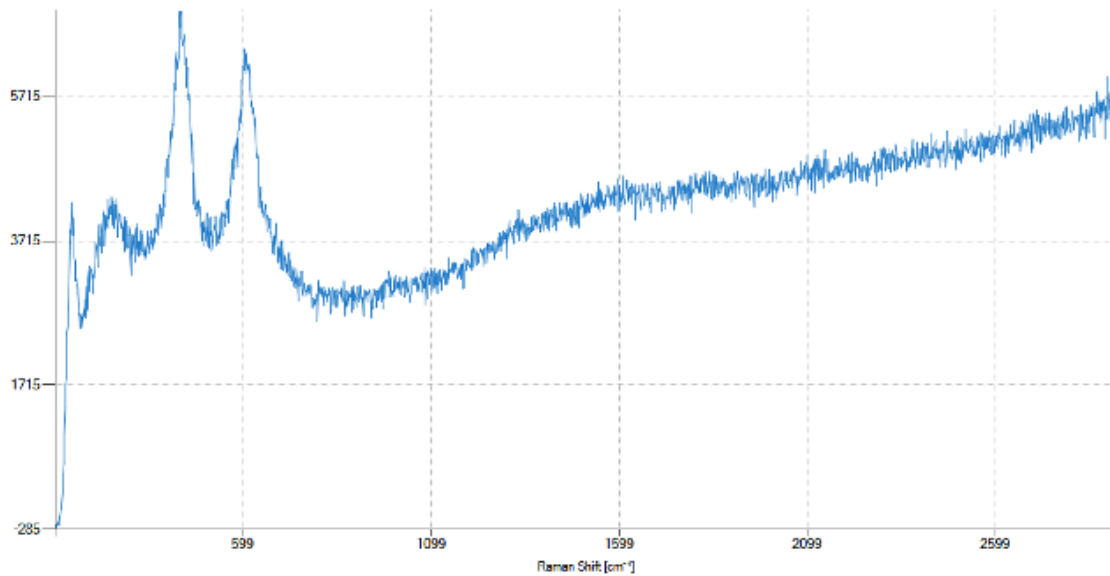


**Fig. 9: Raman Spectroscopy of 1.50wt% Mg doped ZnO thin film**

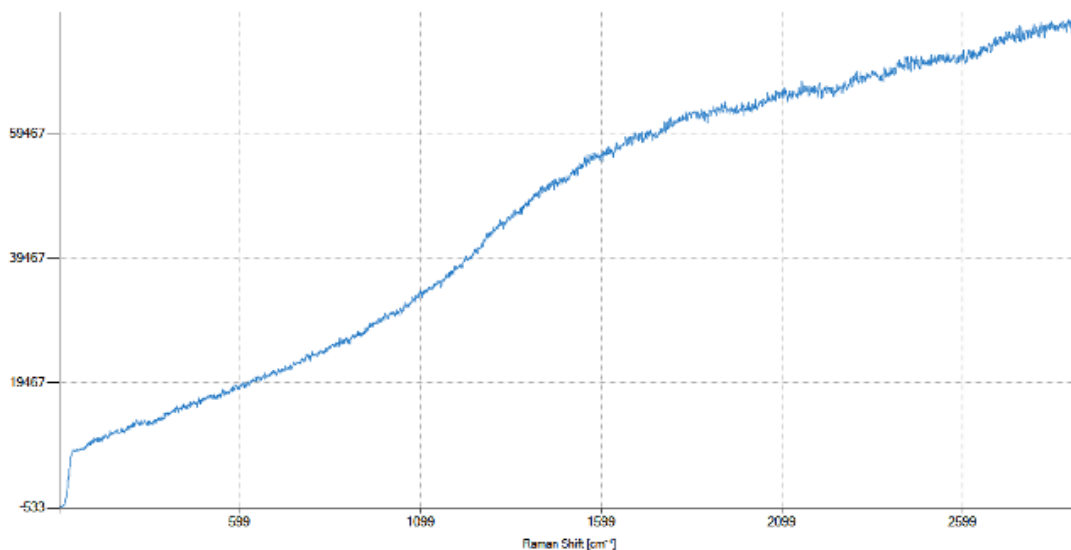


**Fig. 10: Raman Spectroscopy of 2.12wt% Mg doped ZnO thin film**

The above three graphs show the variance in the vibrational and rotational spectra using Raman spectroscopy. In Fig. 9, the strong peaks occur at  $435 \text{ cm}^{-1}$  and  $603 \text{ cm}^{-1}$ , which tell about the vibrational mode, and the small peaks occur at  $144 \text{ cm}^{-1}$  and  $216 \text{ cm}^{-1}$ . In Raman spectrum, the subsequent formula can be used:

$$\Delta\bar{\nu} = \left( \frac{1}{\lambda_0} - \frac{1}{\lambda_1} \right)$$

where  $\Delta\bar{\nu}$  is the Raman shift demonstrated in wave number and  $\lambda_0$  is excitation wavelength, and  $\lambda_1$  is

Raman spectrum wavelength.

### 3.3. SEM Analysis

A scanning electron microscope (SEM) is familiar with producing images of a sample material by scanning the surface by a focused beam of electrons. A sample's surface topography and chemical composition can be determined by using a high-energy beam of electrons interacting with the sample's atoms. Using the beam's position and the intensity of the observed signal, a SEM image of the sample can be created. A secondary electron detector (Everhart-Thornley detector) is used

to detect secondary electrons generated from sample atoms, when they are excited by high energy electron beams in the most common mode of operating SEM. Some high-quality SEM instruments may attain resolutions as high as 1 nanometer or even greater. A schematic diagram of SEM and its function is illustrated in Fig. 11.

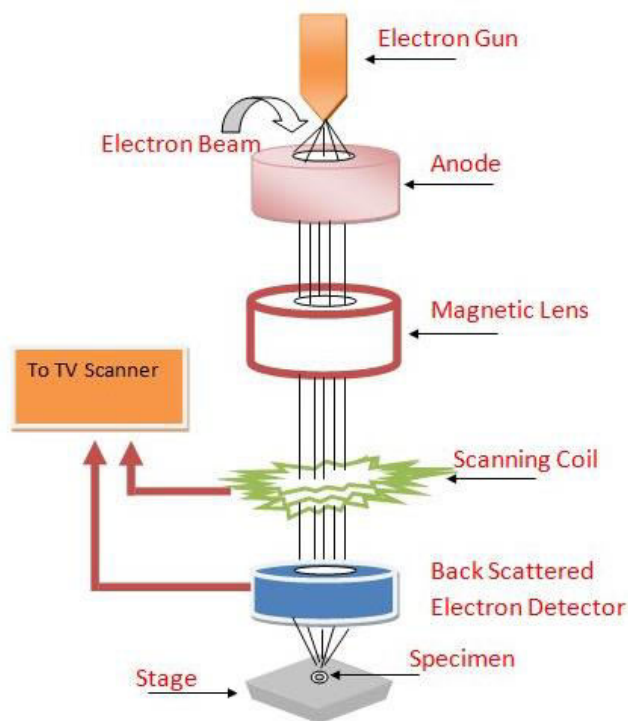


Fig. 11: SEM Spectroscopy Setup

SEM images of Mg-doped ZnO film produced using combination of sol-gel and dip-coating methods are shown in Fig. 12. All films containing Mg-doped ZnO have microstructures of the order of few hundred nanometers with a homogeneous and dense distribution. Incorporation of magnesium results into the formation of a non-uniform surface. The grade of uniformity and roughness depend on the doping concentration of Mg. The grains formed at nano-scale appear to be of spherical shape. These images reveal that thermal annealing at 500°C causes micron size cracks into the film. Thus, we conclude that these micro-size smooth regions are formed by agglomeration of nano-particles. These cracks can be said to be formed because of volume change due to microscale thermal fluctuations which may commonly occur during annealing process of very thin film thickness ranging into the dimensions of nano-micrometer range.

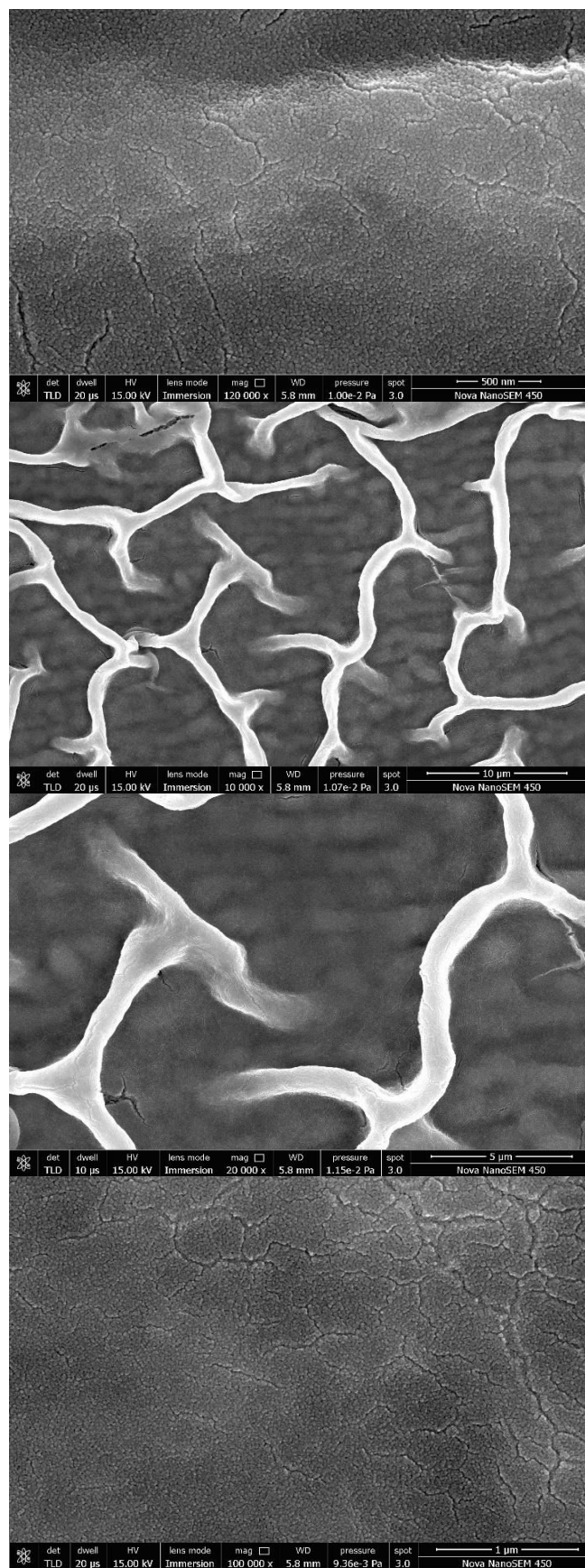


Fig. 12: SEM images of 1.50 wt% Mg-doped ZnO nano-structured film in different magnifications

#### 4. CONCLUSION

Mg-doped ZnO thin films were synthesized in this study using a combination of sol-gel and dip-coating method (DCM), where the dip-coating procedure was repeated many times to expand the film thickness. Variations in optical absorption edges and band gap energy, associated with phase transition or phase separation can be said to be accountable for the changes. Increased Mg content is likely to cause a phase shift. The Raman spectra show that Mg-doped ZnO nano-structured thin films have a more crystalline character than ZnO thin films. On account of the Burstein-Moss phenomenon, the UV absorption-edge of ZnO thin films doped with Mg blueshifts. From SEM analysis, nano-dots or nanocob web-like structures can be seen in the thin films.

#### 5. ACKNOWLEDGEMENTS

The authors are thankful to Material Research Centre (MRC), MNIT, Jaipur for characterization of the samples.

#### Conflict of interest

None declared

#### Source of funding

None declared

#### 6. REFERENCES

- Znaidi L. *Mate. Sci. and Eng : B.*, 2010; **174**:18–30.
- Baruah S, Dutta J. *Sci. and Tech. of Adv. Mate.*, 2009; **10**:013001.
- Kaushal A, Kaur D. *Solar Energy Materials and Solar Cells*, 2009; **93**:193-198.
- Özgür Ü, Alivov Y I, Liu C, Teke A, Reshchikov M A, Doğan S, et. al. *J. of Appl. Phys*, 2005; **98**:041301.
- Sengupta J, Ahmed A, Labar R. *Mate. Lett.*, 2013; **109**:265–268.
- Fang D, Li C, Wang N, Li P, Yao P. *Crys. Rese. and Tech.*, 2013; **48**:265–272.
- Mallika A N, Ramachandra Reddy A, Sowri Babu K, Sujatha C, Venugopal Reddy K. *Optic. Mate.*, 2014; **36**:879–884.
- Dobrozhan O, Diachenko O, Kolesnyk M, Stepanenko A, Vorobiov S, Baláž P, et al. *Mate. Sci. in Semi. Proce.*, 2019; **102**:104595.
- Huang K, Tang Z, Zhang L, Yu J, Lv J, Liu X, et al. *Appl Surf Sci.*, 2012; **258**:3710–3713.
- Hu Y, Cai B, Hu Z, Liu Y, Zhang S, Zeng H. *Curr Appl Phys.*, 2015; **15**:423–428.
- Etacheri V, Roshan R, Kumar V. *ACS Appl. Mater. Interf.*, 2012; **4**:27, 17–25.
- Ghosh R, Basak D. *J. of Appl. Phys.*, 2007; **101**:113111.
- Andriotis AN, Menon M. *J. Appl. Phys.*, 2015; **117**:125708.
- Jiang Z Y, Zhu K R, Lin Z Q, Jin S W, Li G. *Rare Met.*, 2015; doi:10.1007/s12598-015-0505-6
- Tsay CY, Wang MC, Chiang SC. *Mater Trans.*, 2008; **49**:1186–1191.
- Malenovska M, Martinez S, Neouze M A, Schubert U. *Europ. J. of Inor. Chem.*, 2007; **18**:2609–2611.
- Singh AK, Viswanath V, Janu VC. *J. of Lum.*, 2009; **129**:874–878.
- Sowri Babu K, Ramachandra Reddy A, Sujatha C, Reddy KVG, Mallika AN. *Mat. Lett.*, 2013; **110**:10–12.
- Umaralikhan L, Jaffar MJM. *J. of Mate. Sci.: Mat. in Elec.*, 2017; **28**:7677–7685.
- Zhao M, Wang X, Ning L, He H, Jia J, Zhang L, Li X. *J. of Alloy and Comp.*, 2010; **507**: 97–100.
- Zhai WL, Li DW, Qu LL, Fossey JS, Long YT. *Nanosc.*, 2012; **4**:137–142.
- Freire T, Fragoso AR, Matias M, Pinto JV, Marques AC, Pimentel A, et. al. *Nano Express*, 2021; <https://doi.org/10.1088/2632-959X/abed40>
- Wang L, Luo J, Maye MM, Fan Q, Rendeng Q, Engelhard MH, et. al. *J. of Mat. Chem.*, 2005; **15**:1821.
- Chen X, Jia B, Saha JK, Cai B, Stokes N, Qiao, Q et.al. *Nano Letters*, 2012; **12**: 2187–2192.
- Ben-Sasson M, Zodrow K R, Genggeng Q, Kang Y, Giannelis EP, Elimelech M. *Env. Sci. & Tech.*, 2013; **48**:384 – 393.
- Akimov YA, Koh WS, Ostrikov K. *Optics Exp.*, 2009; **12**:10195.